inter·noise 96
25th Anniversary Congress – Liverpool

INCE: 37.7

EFFECT OF THE DIFFERENCE BETWEEN ERROR PATH C AND ITS ESTIMATE $\hat{C}$ FOR ACTIVE NOISE CONTROL USING FILTERED-X LMS ALGORITHM

K Kurisu

TOA Corporation, 2-1 Takamatsu-cho, Takarazuka, 665 Hyogo, Japan

1. INTRODUCTION

The filtered-x LMS algorithm is commonly implemented in active noise control (ANC) (*Fig. 1*). The filter $\hat{C}$ is an estimated transfer function between a secondary source and a error microphone and must be efficiently identified to the actual error path C for effective noise cancellation. In this paper, effects of $\hat{C}$ modelling errors on the performance of ANC are investigated. Several papers [1-3] have already considered this problem and obtained the result that a maximum phase error of $\pm\pi/2$ between C and $\hat{C}$ is the limit for stable ANC. In this paper, however, the same result is derived in a different manner, which can be well understood with intuitive ease. The effect of the phase error is graphically depicted on a complex plane and only a Fourier transformation is employed; this is in contrast to the above stated papers, which use a z-transformation. Theoretically derived results were actually verified through a series of applications to model exhaust ducts of various dimensions.

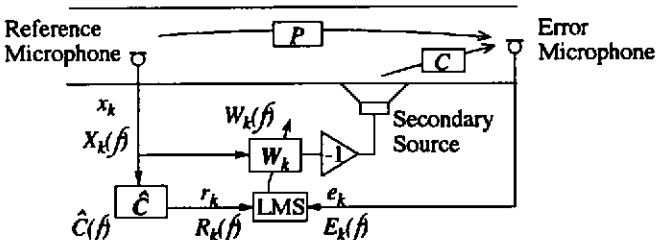

Fig. 1 Schematic view of an ANC system using the filtered-x LMS algorithm

2. RECURSION OF THE TOTAL TRANSFER FUNCTION IN A DUCT

The total transfer function H_k between the reference and error microphone positions and include both acoustical and electrical paths (*Fig. 1*);

$$H_k = P - C W_k , \quad (1)$$

and an adaptation process of W_k by the filtered-x LMS algorithm for frequency domain [4];

$$W_{k+1} = W_k + 2\mu E_k R_k^* , \quad (2)$$

lead

$$H_{k+1} - H_k = - C (W_{k+1} - W_k) = - 2\mu E_k X_k^* C \hat{C}^* , \quad (3)$$

where, μ is the step size parameter (a real number), E_k is the frequency characteristics of the error signal at time k, R_k is the frequency characteristics of the $\hat{C}$ filtered reference input at time k, and the asterisk denotes the complex conjugate. Since the error E_k is considered as the output of the total transfer function H_k for the input X_k,

$$E_k = H_k X_k , \quad (4)$$

the recursive expression of H_k is expressed as

$$H_{k+1} = (1 - 2\mu | X_k |^2 C \hat{C}^*) H_k . \quad (5)$$

When the reference signal X_k is assumed to be static and denoted by X_{av}, we obtain

$$H_k = (1 - 2\mu | X_{av} |^2 C \hat{C}^*)^k H_0 . \quad (6)$$

For stable ANC without an increase of error E_k ($=H_k X_{av}$), the coefficient $(1-2\mu | X_{av} |^2 C\hat{C}^*)$ in *Eq. (5)* and *(6)* must be within the unit circle of the complex plane.

The convergence coefficient $(1-2\mu | X_{av} |^2 C\hat{C}^*)$ of the total transfer function H_k for a complex plane at a given frequency is represented in *Fig. 2*, using exponential expressions.

$$A_1 \exp[j\theta_1] = 1 + A_2 \exp[j(\pi + \theta_2)] \quad (7)$$

$$A_2 \exp[j(\pi + \theta_2)] = - 2\mu | X_{av} |^2 C\hat{C}^* \quad (8)$$

Since μ and $| X_{av} |^2$ are both real, θ_2 denotes the phase angle of $C\hat{C}^*$, i.e., the phase error of $\hat{C}$. In general, μ is set to $\mu \ll 1$ and the maximum value operated in a DSP is normalized to 1. Practical discrimination of which coefficient $(1-2\mu | X_{av} |^2 C\hat{C}^*)$ is within the unit circle can be simplified by using θ_2 and expressed (*Fig. 2*) as

$$- \pi /2 < \theta_2 < \pi /2. \quad (9)$$

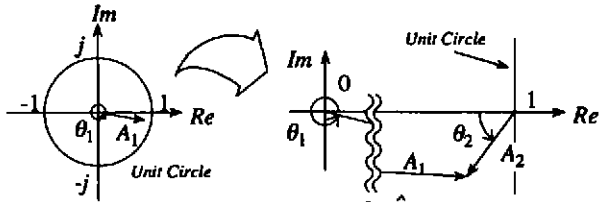

Fig. 2 Convergence coefficient $(1-2\mu | X_{av} |^2 C\hat{C}^*)$ and θ_2 for a complex plane

3. PHASE ANGLE OF $C\hat{C}^*$ AND ANC PERFORMANCES

To examine the relation between characteristics of $C\hat{C}^*$ and ANC performance, the three duct configurations L, M, and S shown in *Fig. 3* were constructed and their error path characteristics C_L, C_M, and C_S were identified as estimates of each error path. *Figure. 4* gives characteristics of the coefficient $(1-2\mu | X_{av} |^2 C\hat{C}^*)$ for a complex plane when C and $\hat{C}$

have the following conditions: a) $\hat{C}=C_L$, $C=C_M$, b) $\hat{C}=C_L$, $C=C_S$, c) $\hat{C}=C_M$, $C=C_S$, where $\mu=0.0005$ and $|X_{av}|=1$.

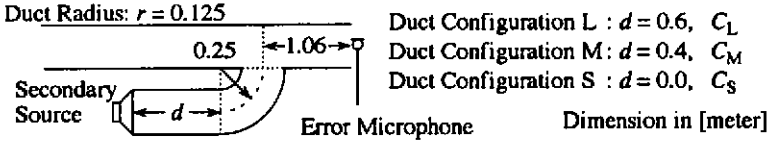

Fig. 3 Experimental duct configurations L, M, and S

For example, condition a) means that the present characteristics of the error path are equal to C_M, but its initial state agreed with C_L. This implies that the equivalent length of the error path is shortened by an increase in sound speed as the duct temperature rises. Active movement of loci around 1 on a complex plane, both inside and outside the unit circle, can been seen (*Fig. 4*).

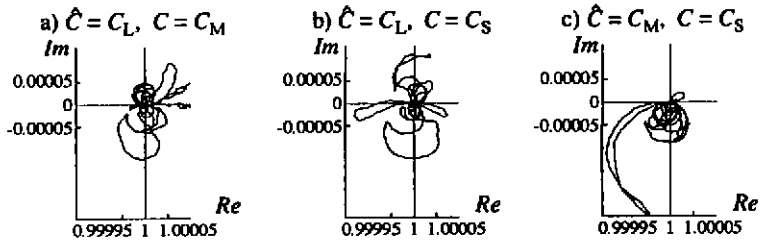

Fig. 4 Loci of the convergence coefficient on a complex plane

The central perpendicular line in each illustration of *Fig. 4* corresponds to the unit circle on a complex plane. Frequency characteristics of θ_2 and the magnitude of the coefficient $(1-2\mu|X_{av}|^2C\hat{C}^*)$, are illustrated in *Fig. 5*. Error signal increases are expected at frequencies where the coefficient $(1-2\mu|X_{av}|^2C\hat{C}^*)$ is outside of the unit circle, i.e., the magnitude of the coefficient exceeds 1 or the phase error θ_2 is over or below $\pm\pi/2$ (*Fig. 5*).

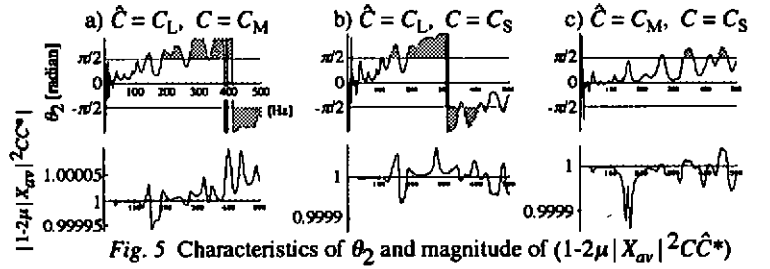

Fig. 5 Characteristics of θ_2 and magnitude of $(1-2\mu|X_{av}|^2C\hat{C}^*)$

Figure. 6 shows frequency characteristics of the resultant error signal when ANC was applied to each duct configuration. In these three ANC experiments, each duct configuration and $\hat{C}$ correspond to the conditions a), b), and c), respectively. For example, a) in *Fig. 6* means that C_L is applied to ANC for the duct with configuration M as its error path.

Significant increases in the error signal can be seen in the same frequency bands shown in *Fig. 5*. The ANC experiments were carried out under the following conditions: the sampling frequency was 3 kHz, the tap lengths of $\boldsymbol{W}_k$ and $\hat{\boldsymbol{C}}$ were 510 and 256, respectively and μ equalled 0.0005; the frequency characteristics of the error signal were measured within 1 minute after ANC operation started.

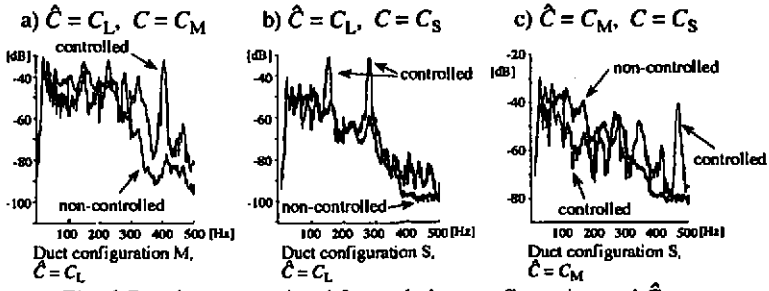

Fig. 6 Resultant error signal for each duct configuration and $\hat{C}$ set

4. CONCLUSIVE REMARKS

A recursive expression for the total transfer function H_k was derived for the case when target noise x_k is static and its frequency spectrum can be expressed as X_{av}. In addition, the admissive condition for avoiding an error signal increases was introduced as *Eq. (9)* in section 2. The result was verified through a series of applications to a model of an actual exhaust duct.

Over the last few years, several studies [1-3] related to this phase condition have been made and arrived at the same conclusion as *Eq. (9)*. The manner of derivation in this paper, however, seems to be valid in the sense of that it is quite easy to understand the roles of $\hat{C}$ and its phase angle by depicting them on the complex plane shown in section 2. This is because only expressions for frequency characteristics and related arithmetic have been employed in this paper.

Acknowledgements

The author would like to express his gratitude to Dr. Hiroshi KANAI of Tohoku Univ., Japan, Mr. Yoshinobu KAJIKAWA of Kansai Univ., Japan, and Mr. Akira OMOTO of Kyushu Inst. of Design, Japan, for their helpful comments and kind suggestions.

References

[1] S.J.Elliott, I.M.Stothers, P.A.Nelson, IEEE Trans Acoust Speech Signal Process, vol. 35, no. 10, pp. 1423-1434 (1987).

[2] C.C.Bouche, S.J.Elliott, P.A.Nelson, IEE Proc Part F, vol. 138, no. 4, pp. 313-319 (1991).

[3] S.D.Snyder, C.H.Hansen, IEEE Trans Signal Process, vol. 42, no. 4, pp. 950-953 (1994).

[4] G.Chen, M.Abe, T.Sone, J. Acoust. Soc. Jpn(E), vol. 16, no. 6, pp. 331-340 (1995).